ISSN (Print) 1226-1750
ISSN (Online) 2233-6656
Journal of Magnetics 25(1), 8-14 (2020) https://doi.org/10.4283/JMAG.2020.25.1.008

Theoretical Investigations of Entropy Optimization in Electro-Magneto Nonlinear Mixed Convective Second Order Slip Flow

M. Ijaz Khan[1]*, Sumaira Qayyum[2], S. Kadry[3], W. A. Khan[4,5], and S. Z. Abbas[4,6]

[1]*Department of Mathematics, Riphah International University, Faisalabad Campus, Faisalabad, 38000 Pakistan*
[2]*Department of Mathematics, Quaid-I-Azam University 45320, Islamabad 44000, Pakistan*
[3]*Department of Mathematics and Computer Science, Faculty of Science, Beirut Arab University, Lebanon*
[4]*School of Mathematics and Statistics, Beijing Institute of Technology, Beijing 100081, China*
[5]*Department of Mathematics, Mohi-ud-Din Islamic University, Nerian Sharif, 12010 Azad Kashmir, Pakistan*
[6]*Department of Mathematics and Statistics, Hazara University Mansehra, KPK, Pakistan*

(Received 24 August 2019, Received in final form 12 February 2020, Accepted 10 March 2020)

Here nonlinear mixed convective entropy based nanofluid second order slip flow of magnetic and electric field is addressed. Both electric and magnetic field is considered for the problem formulation and the flow is generated by a stretched surface. Important slip factors, i.e., Brownian and thermophoresis diffusions are accounted. Total entropy rate subject to four types of irreversibilities (i) heat transfer (ii) chemical reaction (iii) fluid friction (iv) Joule or Ohmic heating is obtained through second law of thermodynamics. Thermal radiation, heat generation/absorption, dissipation, Brownian motion, Joule or Ohmic heating and thermophoresis effects are considered in the development of the energy equation. Activation energy to undergo the physical transportation or chemical transformation of atoms or molecules is further considered in the analysis of concentration. Firstly ordinary differential system is found, then numerically solved for flow field, entropy generation, concentration, temperature, skin friction, Nusselt number, Bejan number and Sherwood number through built-in-Shooting method.

Keywords : nonlinear mixed convection, second order velocity slip, activation energy, magnetic and electric field, thermal radiation, entropy generation.

1. Introduction

Thermal system optimization has gained a meaningful consideration of researchers and investigators in the last couple of years owing to the need of minimizing pinnacle temperature and entropy rate for effective execution of the system. The search for accomplishing an advanced thermal system has persuaded the analysts to scrutinize diverse accompanying elements that are capable in dictating the temperature achieved and irreversibilities brought about inside the system. Analysts have confirmed in the process, that frequent factors like thermo-physical characteristics of materials, geometrical configuration and some other passive considerations, for example baffles, mediate the optimality of thermal field and entropy rate of system to important extent. A lot of investigations on entropy optimization in different liquid flow circumstances have been done by researchers and engineers concentrating on entropy optimization. These researches are motivated by the significance of irreversibility in liquid flows and their usage in numerous mechanical and industrial applications such as in thermal processes like refrigerators, air conditioners, combustion engines, pumps, and so forth others. Some valuable irreversible processes in fluid dynamics comprise fluid viscosity, Joule heating, liquid flow via resistive medium like Joule-Thomson impact and diffusion, heat generation via thermal resistance and so on. Due to such occurrence, numerous researchers have focused on the importance of entropy generation in fluid flow subject to different flow geometries. Lopez *et al.* [1] examined entropy generation and heat transfer in MHD flow of aluminium-water subject to nonlinear radiative heat flux in a porous vertical microchannel. The combined behaviors of magnetic field, hydrodynamic slip, nanoparticles volume friction, thermal radiation and suction/injection on entropy optimization and heat transport were investigated. The

*Corresponding author: Tel: +923009019713
Fax: +923409019713, e-mail: mikhan@math.qau.edu.pk

governing dimensionless expressions were numerically tackled through implementation of the Runge-Kutta method along with Shooting technique. The obtained outcomes for accuracy are compared with literatures. Sithole *et al.* [2] investigated magnetohydrodynamic entropy generation in nanomaterial flow of second grade liquid with dissipation and radiative heat flux towards a convectively heated surface. The non-Newtonian liquid is considered electrically conducting. The results are computed for flow field and temperature distribution via spectral local linearization technique. Ahmed *et al.* [3] scrutinized double diffusive entropy optimized convective flow of non-Newtonian material (Casson fluid) with slip conditions towards nonlinear stretched surface. The behavior of concentration field is discussed through first order chemical reaction. It is witnessed from the obtained results that velocity and temperature of material particles boost versus higher estimations of Casson parameter. Muhammad *et al.* [4, 5] explored entropy generation over a curved surface with magnetohydrodynamics, second order velocity slip, thermal radiation, homogeneous-heterogeneous reactions, Joule heating, Darcy-Forchheimer, viscous dissipation, mixed convection, activation energy and convective boundary conditions. The results are obtained via the built-In-Shooting method for velocity, temperature, concentration, entropy generation rate, skin friction, Bejan number and Nusselt number and displayed graphically. Refs. [6-12] highlights the flow of nanofluids.

In the last few decades, engineers and investigators have been focused to enhance the hydrothermal execution of mechanical and industrial systems by means of utilizing nanoscale devices like MEMs, NEMs, electronic devices, and etcetera has been the focus of consideration amongst the analyst all around the globe [11-15]. Scattering metal or non-metal nanomaterials in various continuous phase liquids like ethylene glycol $(CH_2OH)_2$ and water (H_2O) develops a hybrid named called nanofluid subject to the homogenous circulation of nanoparticles. Enhancing the thermal performance of nanomaterials causes developed thermal performance of mixture fluid as well. Therefore, utilizing nanoliquids outcomes in a heat transport augmentation via the mixture combined with its convective heat transport intensification because of Brownian motions of nanoparticles. Initially, Buongiorno's [16] gave the concept of seven slip mechanisms i.e., fluid drainage, thermophoresis, Magnus effect, Brownian diffusion, inertia, gravity and diffusionphoresis. He concluded that from these seven slip mechanisms that thermophoresis and Brownian diffusion are important slip mechanisms in nanoliquids. Therefore, we have considered Brownian motion and thermophoresis diffusion effects of nanofluid for the enhancement of thermal conductivity of base fluid. Some fruitful studies on heat transport towards different flow geometries can be seen in Refs. [17-22].

In the current research article, we have theoretical discussed the impact of Brownian motion and thermophoresis diffusion in nonlinear mixed convective entropy based flow of magnetic and electric field over a stretched surface. The second order velocity slip effect is considered as the boundary of stretched surface. The energy equation is developed with heat generation, thermal radiation, Brownian motion, dissipation, thermophoresis and Ohmic heating. Firstly ordinary differential system is found, then numerically solved for flow field, entropy generation, concentration, temperature, skin friction, Nusselt number, Bejan number and Sherwood number through built-in-Shooting method.

2. Modeling

The combined effects of magnetic and electric field is considered for the analysis of fluid flow over a stretched surface of sheet with nonlinear mixed convection, second order velocity slip and magnetohydrodynamics. The flow behavior is discussed in the region $(y > 0)$. Let us assumed that $u_w(x)$ is the stretching velocity along x–axis and the deformation in fluid along y–axis where $(b > 0)$ and represents the stretching rate. Fig. 1 is sketched for the graphical representation of flow description. After imple-

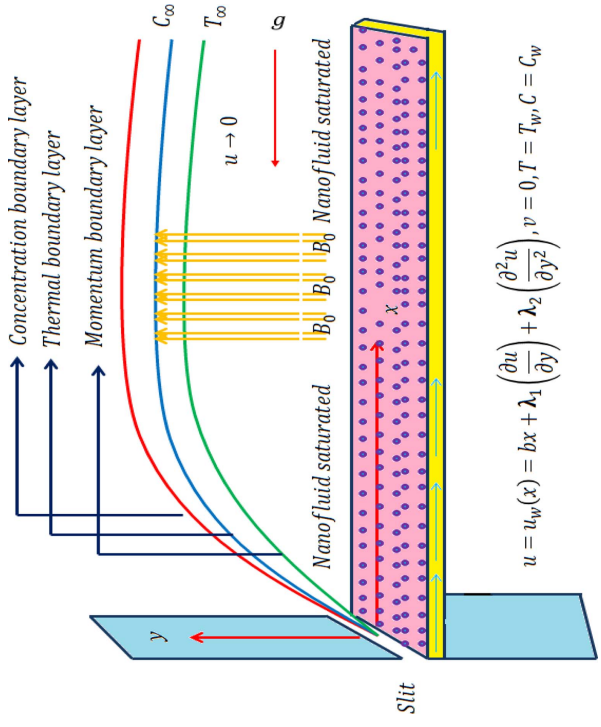

Fig. 1. (Color online) Flow diagram.

menting the concept of boundary layer approximations, we have the following flow expressions [4, 5]:

$$\frac{\partial u}{\partial x}+\frac{\partial v}{\partial y}=0, \tag{1}$$

$$\left.\begin{aligned} u\frac{\partial u}{\partial x}+v\frac{\partial u}{\partial y}=-\frac{1}{\rho_f}\frac{\partial p}{\partial x}+\nu_f\frac{\partial^2 u}{\partial y^2}+\frac{\sigma}{\rho_f}(E_0B_0-B_0^2u)\\ +g(\beta_1(T-T_\infty)+\beta_2(T-T_\infty)^2+\beta_3(C-C_\infty)+\beta_4(C-C_\infty)^2),\end{aligned}\right\} \tag{2}$$

$$\left.\begin{aligned} u\frac{\partial T}{\partial x}+v\frac{\partial T}{\partial y}=\alpha\frac{\partial^2 T}{\partial y^2}+\frac{\mu_f}{(\rho c_p)_f}\left(\frac{\partial u}{\partial y}\right)^2\\ +\tau\left(D_B\frac{\partial C}{\partial y}\frac{\partial T}{\partial y}+\frac{D_T}{T_\infty}\left(\frac{\partial T}{\partial y}\right)^2\right)+\frac{\sigma}{(\rho c_p)_f}(uB_0-E_0B_0)^2\\ +\frac{Q_0}{(\rho c_p)_f}(T-T_\infty)+\frac{16\sigma^*T_\infty^3}{3k^*}\frac{\partial^2 T}{\partial y^2},\end{aligned}\right\} \tag{3}$$

$$u\frac{\partial C}{\partial x}+v\frac{\partial C}{\partial y}=D_B\frac{\partial^2 C}{\partial y^2}+\frac{D_T}{T_\infty}\frac{\partial^2 T}{\partial y^2} -k_r^2(C-C_\infty)\left(\frac{T}{T_\infty}\right)^n\exp\left[\frac{-E_a}{\kappa T}\right], \tag{4}$$

with

$$\left.\begin{aligned} u=u_w(x)=bx+\lambda_1\left(\frac{\partial u}{\partial y}\right)+\lambda_2\left(\frac{\partial^2 u}{\partial y^2}\right),\\ v=0,\ T=T_w,\ C=C_w \text{ at } y=0,\\ u\to 0,\ T\to T_\infty,\ C\to C_\infty \text{ when } y\to\infty.\end{aligned}\right\} \tag{5}$$

Implementing the following transformations

$$\left.\begin{aligned} u=bxf'(\xi),\ \ v=-\sqrt{b\nu_f}\,f(\xi),\ \ \theta(\xi)=\frac{T-T_\infty}{T_w-T_\infty},\\ \phi(\xi)=\frac{C-C_\infty}{C_w-C_\infty},\ \ \xi=\sqrt{\frac{b}{\nu_f}}y.\end{aligned}\right\} \tag{6}$$

We arrive to the following dimensionless equations

$$f'''+ff''-f'^2+M(E_1-f')+\lambda\theta(1+\beta_t\theta) +\lambda N^*\phi(1+\beta_c\phi)=0, \tag{7}$$

$$(1+R)\theta''+\Pr f\theta'+\Pr(Nb\theta'\phi'+Nt\theta'^2) +Br(f''^2+M(f'^2-E_1)^2)+\Pr\beta\theta=0, \tag{8}$$

$$\phi''+Scf\phi'+\left(\frac{Nt}{Nb}\right)\theta''-k_1Sc\phi(1+\alpha_1\theta)^n\exp\left(\frac{-E^*}{1+\alpha_1\theta}\right)=0, \tag{9}$$

with

$$\left.\begin{aligned} f(0)=0,\ f'(0)=1+L_1f''(0)+L_2f'''(0),\ \theta(0)=1,\ \phi(0)=1,\\ f'(\infty)=0,\ \theta(\infty)=0,\ \phi(\infty)=0.\end{aligned}\right\} \tag{10}$$

In the above expressions $M\left(=\frac{\sigma B_0^2}{b\rho_f}\right)$ shows magnetic parameter, $E_1\left(=\frac{E_0}{B_0u_w}\right)$ electric field parameter, $\lambda\left(=\frac{Gr}{\mathrm{Re}^2}\right)$ mixed convection parameter, $Gr\left(=\frac{g\beta_1(T_w-T_\infty)x^3}{\nu_f^2}\right)$ Grashof number, $\mathrm{Re}\left(=\frac{u_wx}{\nu_f}\right)$ local Reynolds number, $N^*\left(=\frac{\beta_3(C_w-C_\infty)}{\beta_1(T_w-T_\infty)}\right)$ buoyancy ratio variable, $\Pr\left(=\frac{\nu_f}{\alpha}\right)$ Prandtl number, $Nt\left(=\frac{\tau D_T(T_w-T_\infty)}{T_\infty\nu_f}\right)$ thermophoresis variable, $Br\left(=\Pr.Ec\right)$ Brinkman number, $Ec\left(=\frac{(bx)^2}{c_p(T_w-T_\infty)}\right)$ Eckert number, $Nb\left(=\frac{\tau D_B(C_w-C_\infty)}{\nu_f}\right)$ Brownian motion variable, $\left(\beta_t=\frac{\beta_2(T_w-T_\infty)}{\beta_1}\right)$, $\left(\beta_c=\frac{\beta_4(C_w-C_\infty)}{\beta_3}\right)$ nonlinear convection variables subject to temperature and concentration, $\left(R=\frac{16\sigma^*T_\infty^3}{3k_fk^*}\right)$ radiation parameter, $E^*\left(=\frac{E_a}{\kappa T_\infty}\right)$ activation energy variable, $\beta\left(=\frac{Q_0}{b(\rho c_p)_f}\right)$ heat generation/absorption variable, $\left(\alpha_1=\frac{(T_w-T_\infty)}{T_\infty}\right)$ temperature ratio variable, $\left(L_1=\lambda_1\sqrt{\frac{b}{\nu_f}}\right)$, $L_2=\frac{\lambda_2 b}{\nu_f}$ first and second order slip variables, $Sc\left(=\frac{\nu_f}{D_B}\right)$ Schmidt number and $k_1\left(=\frac{k_r^2}{b}\right)$ chemical reaction parameter.

3. Engineering Impact

Mathematically, the C_{fx}, Nu_x and Sh_x are defined as

$$C_{fx}=\frac{\tau_w}{\frac{1}{2}\rho_f(u_w)^2},\ Nu_x=\frac{xq_w}{k_f(T_w-T_\infty)},\ Sh_x=\frac{xj_w}{D_B(C_w-C_\infty)}, \tag{11}$$

where Nu_x Nusselt number, C_{fx} indicates the skin friction coefficient, q_w heat flux, Sh_x Sherwood number, τ_w shear stress and j_w mass flux. Mathematically, τ_w, q_w and j_w are addressed as

$$\tau_w=\left(\mu_f\frac{\partial u}{\partial y}\right)_{y=0},\ q_w=-k_f\left[1+\frac{16\sigma^*T_\infty^3}{3k^*k_f}\right]\left(\frac{\partial T}{\partial y}\right)_{y=0}, \quad j_w=-D_B\left(\frac{\partial C}{\partial y}\right)_{y=0}, \tag{12}$$

invoking Eq. (12) in Eq. (11), one has

$$C_{fx}\,\mathrm{Re}^{0.5}=f''(0),\ Nu_x\,\mathrm{Re}^{-0.5}=-(1+R)\theta'(0), \quad Sh_x\,\mathrm{Re}^{-0.5}=-\phi'(0). \tag{13}$$

4. Mathematical Modeling of Entropy

In the presence of above assumptions entropy equation is addressed as

$$\left.\begin{aligned} S_g=\frac{k_f}{T_\infty^2}\left(1+\frac{16\sigma^*T_\infty^3}{3k_fk^*}\right)\left(\frac{\partial T}{\partial y}\right)^2+\frac{\mu_f}{T_\infty}\left(\frac{\partial u}{\partial y}\right)^2+\frac{\sigma}{T_\infty}(uB_0-E_0B_0)^2\\ +\frac{R^*D}{C_\infty}\left(\frac{\partial C}{\partial y}\right)^2+\frac{R^*D}{T_\infty}\frac{\partial C}{\partial y}\frac{\partial T}{\partial y}.\end{aligned}\right\} \tag{14}$$

After implementation of Eq. (6), we have the following final form

$$N_G=\alpha_1(1+R)\theta'^2+Brf''^2+MBr(f'-E_1)^2 +L\left(\theta'\phi'+\frac{\alpha_2}{\alpha_1}\phi'^2\right). \tag{15}$$

The Bejan number is

$$Be = \frac{\alpha_1(1+R)\theta'^2 + L\left(\theta'\phi' + \frac{\alpha_2}{\alpha_1}\phi'^2\right)}{\alpha_1(1+R)\theta'^2 + Brf''^2 + MBr(f'-E_1)^2 + L\left(\theta'\phi' + \frac{\alpha_2}{\alpha_1}\phi'^2\right)}. \quad (16)$$

Note that $N_G\left(=\frac{S_g\nu_f T_\infty}{k_f b(T_w - T_\infty)}\right)$ denotes entropy generation rate, $\alpha_2\left(=\frac{C_w - C_\infty}{C_\infty}\right)$ concentration difference variable and $L\left(=\frac{R^* D(C_w - C_\infty)}{k}\right)$ diffusive parameter.

5. Discussion

This section is designed to analyze the behaviors of different variables on velocity, entropy generation, temperature, concentration, Bejan number, skin friction, Sherwood number and Nusselt number (See Figs. 2-16). Figs. 2 and 3 are showing the impact of first (L_1) and second order ($L_2 < 0$) slip parameters on velocity field. Here decrease in motion of the fluid is seen for higher slip parameters (L_1 = 0, 0.2, 0.4, 0.6, 0.8) and (L_2 = 0, –0.4, –0.8, –1.2, –1.6) Physically it is due to reason that when we increase slip parameters stretching velocity does not transfer its effect completely to the fluid so $f'(\xi)$ decays. Fig. 4 displays the influence of Eckert number (Ec) on temperature distribution ($\theta(\xi)$) It is witnessed from the figure that temperature is increasing function of Eckert number (Ec = 0.0, 1.0, 2.0, 3.0, 4.0). Total internal energy of the system boosts up for rising Ec that is why ($\theta(\xi)$) increases. Thermophoresis parameter (Nt) impact on temperature field is seen in Fig. 5. For higher estimation of (Nt = 0, 1.0, 2.0, 3.0, 4.0) temperature shows increasing behavior because temperature difference enhances for larger Nt. Impact of activation energy along concentration field is seen in Fig. 6. It is shown in the figure that activation energy enhances the concentration of the fluid. Here concentration distribution ($\phi(\xi)$) boosts up for higher (E^* = 0.0, 1.0, 2.0, 3.0, 4.0) Fig. 7 shows the opposite behavior of concentration field against chemical reaction parameter (k_1 = 0.0, 0.1, 0.2, 0.3, 0.4). Figs. (8-11) describe the impact of first and second order velocity slip parameters (L_1 and $L_2 < 0$) of entropy generation (N_G)

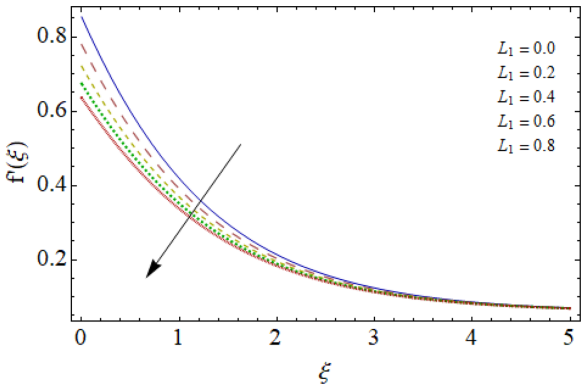

Fig. 2. (Color online) $f'(\xi)$ against L_1.

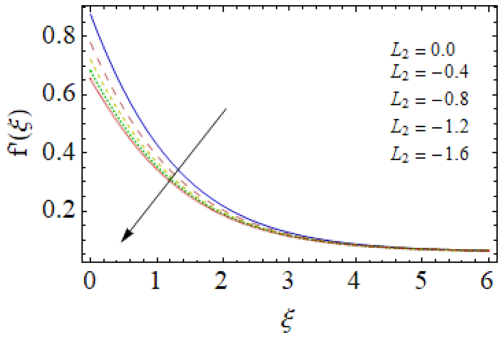

Fig. 3. (Color online) $f'(\xi)$ against L_2.

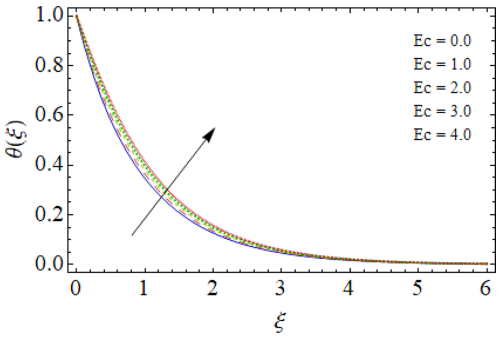

Fig. 4. (Color online) $\theta(\xi)$ against Ec.

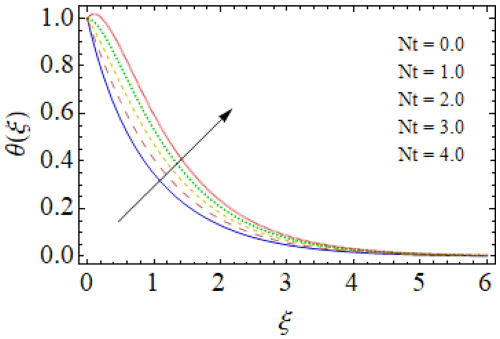

Fig. 5. (Color online) $\theta(\xi)$ against Nt.

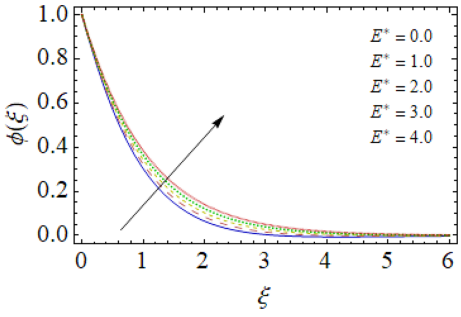

Fig. 6. (Color online) $\phi(\xi)$ against E^*.

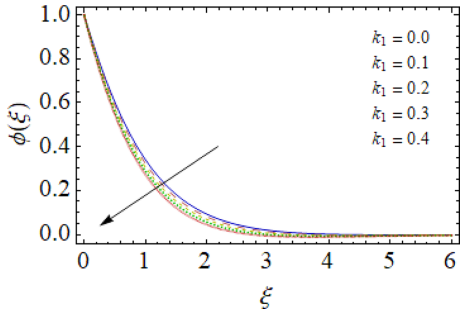

Fig. 7. (Color online) $\phi(\xi)$ against k_1.

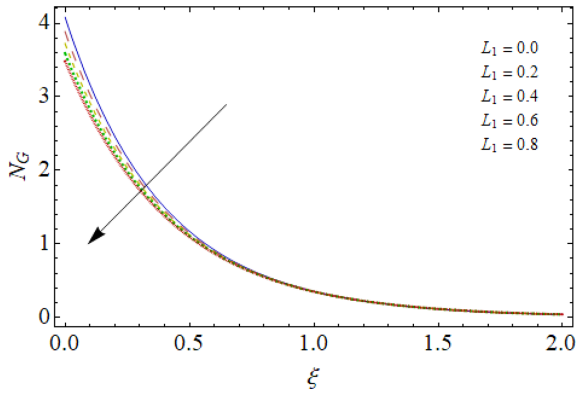

Fig. 8. (Color online) $N_G(\xi)$ against L_1.

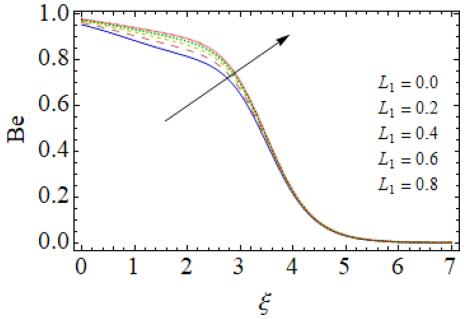

Fig. 9. (Color online) *Be* against L_1.

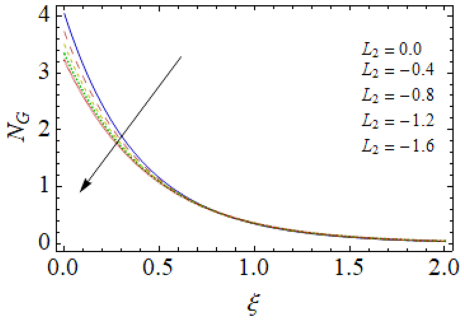

Fig. 10. (Color online) $N_G(\xi)$ against L_2.

and Bejan number (*Be*). It is observed that entropy generation is less for both higher (L_1 and $L_2 < 0$) (see Figs. 8 and 10). However Bejan number shows increasing

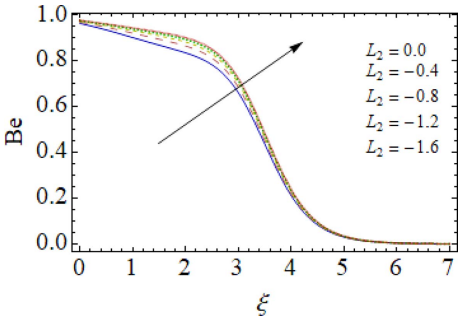

Fig. 11. (Color online) *Be* against L_2.

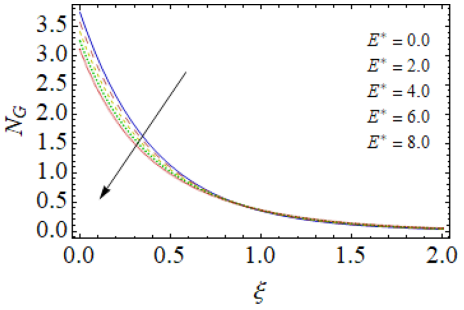

Fig. 12. (Color online) $N_G(\xi)$ against E^*.

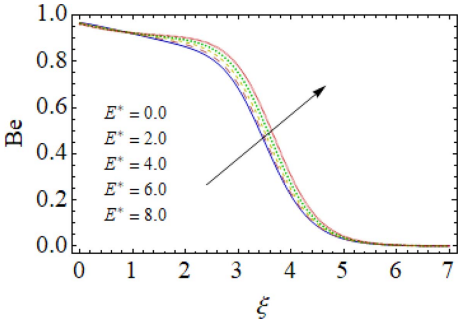

Fig. 13. (Color online) *Be* against E^*.

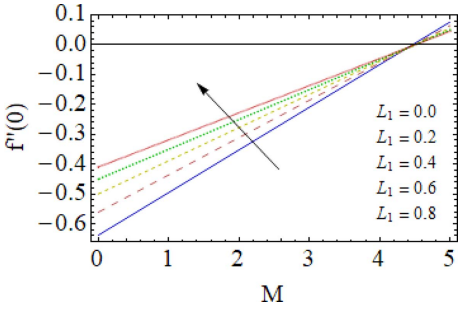

Fig. 14. (Color online) $f''(0)$ against M and L_1.

trend against first and second order slip parameters (L_1 and $L_2 < 0$) (see Figs. 9 and 11). Activation energy (E^*) impact on entropy generation and Bejan number is portrayed in Figs. 12 and 13. Here decrease in irreversibility of the system is noticed for higher ($E^* = 0$, 2.0, 4.0, 6.0,

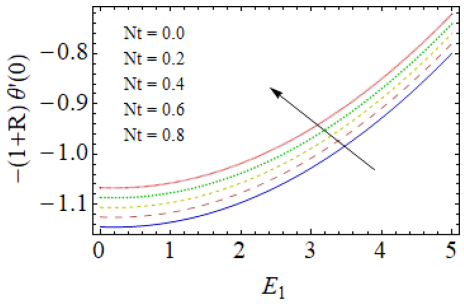

Fig. 15. (Color online) $-(1+R)\theta''(0)$ against Nt and E_1.

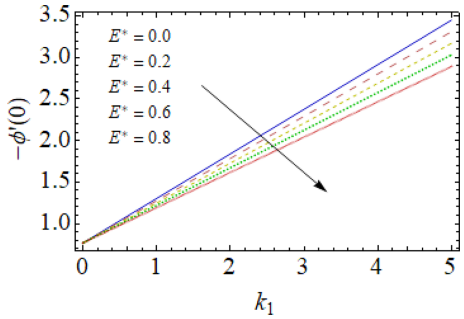

Fig. 16. (Color online) $-\phi'(0)$ against E^* and k_1.

8.0) (see Fig. 12) while Bejan number shows increasing trend (see Fig. 13). Fig. 14 sketches the impact of L_1 and M on surface drag force. Here it is observed that magnitude of $f''(0)$ decays for rising values of L_1 and M. Impact of Nt and E_1 on Nusselt number is seen in Fig. 15. Here also decrease in Nusselt number is noticed for greater Nt and E_1. Fig. 16 discusses the impact of activation energy (E^*) and chemical reaction parameter (k_1) on Sherwood number. Here magnitude of Sherwood number decays for greater (E^*) while shows an increasing trend for (k_1).

6. Conclusions

The main conclusions are given below

- Velocity is decaying for greater (L_1 and $L_2 < 0$).
- Temperature enhances for (Ec).
- Total entropy of the system is decreasing function of slip parameters (L_1 and $L_2 < 0$).
- Bejan number enhances against slip parameter and activation energy.
- Skin friction is less for higher L_1.
- Heat and mass transfer rates are decreasing for larger values of Nt and E^*.

Nomenclature

$u, v\left[\frac{\bar{L}}{\bar{T}}\right]$: velocity components

$g\left[\frac{\bar{L}}{\bar{T}^2}\right]$: Gravity

$\rho\left[\frac{M}{\bar{L}^3}\right]$: Density

$x, y\left[\bar{L}\right]$: Cartesian coordinate

$p\left[\frac{M}{\bar{L}\bar{T}^2}\right]$: Pressure

$E_0\left[\frac{M\bar{L}}{\bar{T}^3 A}\right]$: strength of electric field

$\nu\left[\frac{\bar{L}^2}{\bar{T}}\right]$: kinematic viscosity

$\sigma\left[\frac{\bar{T}^3 A^2}{M\bar{L}^3}\right]$: electrical conductivity

$T, T_w, T_\infty\left[Kelvin\right]$: temperature of the fluid, sheet temperature, ambient temperature

$\beta_1\left[\frac{1}{Kelvin}\right], \beta_2\left[\frac{1}{(Kelvin)^2}\right], \beta_3[1], \beta_4[1]$: linear/nonlinear thermal and concentration expansion coefficients

$D_B\left[\frac{\bar{L}^2}{\bar{T}}\right]$, $D_T\left[\frac{\bar{L}^2}{\bar{T}}\right]$: Brownian diffusion coefficient and thermophoretic diffusion coefficient

$k_f\left[\frac{M\bar{L}}{\bar{T}^3(Kelvin)}\right]$: thermal conductivity

$(\rho c_p)_f, (\rho c_p)_p\left[\frac{M}{\bar{T}^3(Kelvin)\bar{L}}\right]$: heat capacitance of base fluid and nanoparticles

$C, C_w, C_\infty[1]$: concentration of the fluid, sheet concentration, ambient concentration

$Q_0\left[\frac{M}{\bar{T}^4(Kelvin)\bar{L}}\right]$: coefficient of heat generation/absorption,

$\sigma^*\left[\frac{J}{\bar{L}^2\bar{T}(Kelvin)^4}\right], k^*\left[\frac{1}{\bar{L}}\right]$: mean absorption coefficient

$k_r\left[\frac{1}{\sqrt{\bar{T}}}\right]$: reaction rate

$n[1]$: fited rate constant

$\frac{E_a}{\kappa}\left[Kelvin\right]$: activation energy coefficient, Boltzman constant i.e., $\kappa = 8.61 \times 10^{-5}$ eV/K

$u_w\left[\frac{\bar{L}}{\bar{T}}\right]$: stretching velocity

$b\left[\frac{1}{\bar{T}}\right]$: dimensional constant or stretching rate

$\lambda_1[\bar{L}], \lambda_2[\bar{L}^2]$: first and second order velocity slip coefficient

M : magnetic parameter

E_1, Pr : electric field parameter, Prandtl number

λ, Nt : mixed convection parameter, thermophoresis variable

Gr, Br: Grashof number, Brinkman number

Re, Ec: local Reynolds number, Eckert number

N^*, Nb: buoyancy ratio variable, Brownian motion variable

β_t, β_c : nonlinear convection variables subject to temperature and concentration

R, β : radiation parameter, heat generation/absorption variable

E^* : activation energy variable
α_1 : temperature ratio variable
L_1, L_2 : first and second order slip variables
Sc, k_1 : Schmidt number, chemical reaction parameter
Nu_x : Nusselt number
C_{fx}, Sh_x : skin friction coefficient, Sherwood number
$q_w\left[\frac{M}{\bar{T}^3}\right], \tau_w\left[\frac{N}{\bar{L}^2}\right]$: heat flux, shear stress
$j_w\left[\frac{\bar{L}}{\bar{T}}\right]$: mass flux
$S_g\left[\frac{M}{\bar{L}\bar{T}^3(Kelvin)}\right], \alpha_2$: entropy coeficient, concentration difference variable
$R^*\left[\frac{M}{\bar{L}\bar{T}^2(Kelvin)}\right], D\left[\frac{\bar{L}^2}{\bar{T}}\right]$: gas constant, diffusion rate
N_G, L : entropy generation rate, diffusive parameter

References

[1] A. López, G. Ibáñez, J. Pantoja, J. Moreira, and O. Lastres, Int. J. Heat Mass Transf. **107**, 994 (2017).
[2] H. Sithole, H. Mondal, and P. Sibanda, Results Phys. **9** 1085 (2018).
[3] S. E. Ahmed, M. A. Mansour, A. Mahdy, and S. S. Mohamed, Eng. Sci. Techno., An. Int. J. **20**, 1562 (2017).
[4] R. Muhammad, M. I. Khan, N. B. Khan, and M. Jameel, Comput. Meth. Prog. Biomed. **189**, 105294 (2020).
[5] R. Muhammad, M. I. Khan, M. Jameel, and N. B. Khan, Comput. Meth. Prog. Biomed. **188**, 105298 (2020).
[6] M.M. Rashidi, F. Mohammadi, S. Abbasbandy, and M. S. Alhuthali, J. Appl. Fluid Mech. **8**, 765 (2015).
[7] T. Hayat, M. I. Khan, T. A. Khan, M. I. Khan, S. Ahmad, and A. Alsaedi, J. Mol. Liq. **265**, 638 (2018).
[8] M. M. Bhatti, T. Abbas, M. M. Rashidi, M. El-Sayed Ali, and Z. Yang, Entropy **18**, 224 (2016).
[9] T. Hayat, M. I. Khan, S. Qayyum, and A. Alsaedi, Colloid. Surf. A: Physicochem. Eng. Aspect. **539**, 346 (2018).
[10] T. Armaghani, A. Kasaeipoor, N. Alavi, and M. M. Rashidi, J. Mol. Liq. **223**, 251 (2016).
[11] T. Hayat, M. I. Khan, S. Qayyum, A. Alsaedi, and M. I. Khan, Phys. Lett. A **382**, 760 (2018).
[12] M. M. Rashidi, S. Bagheri, E. Momoniat, and N. Freidoonimehr, Ain Sham. Eng. J. **8**, 85 (2017).
[13] M. Ramezanizadeh, M. A. Nazari, M. H. Ahmadi, and E. Açkkalp, J. Mol. Liq. **272**, 402 (2018).
[14] Abdollahi, H. A. Mohammed, S. M. Vanaki, and R. N. Sharma, Ain Sham. Eng. J. **9**, 3418 (2018).
[15] T. Hayat, S. Qayyum, M. I. Khan, and A. Alsaedi, Int. J. Hydrogen Energy **42**, 29120 (2017).
[16] J. Buongiorno, ASME J. Heat Transf. **128**, 250 (2006).
[17] T. Hayat, S. Ahmad, M. I. Khan, and A. Alsaedi, Physica B: Cond. Matt. **537**, 126 (2018).
[18] S. Ahmad, M. Farooq, A. Anjum, and S. Sheriff, J. Magnet. **24**, 697 (2019).
[19] M. Javed, M. Farooq, S. Ahmad, and A. Anjum, J. Magn. **24**, 211 (2019).
[20] M. I. Khan, M. Waqas, T. Hayat, and A. Alsaedi, J. Colloid Interface Sci. **498**, 85 (2017).
[21] T. Hayat, M. I. Khan, M. Farooq, A. Alsaedi, M. Waqas, and T. Yasmeen, Int. J. Heat Mass Transf. **99**, 710 (2016).
[22] M. Waqas, J. Magn. Magn. Mater. **493**, 165646 (2020).